SPECIAL ISSUE-LETTER

Increasing dominance of terrigenous organic matter in circumpolar freshwaters due to permafrost thaw

Maxime Wauthy [ID],[1,2]* Milla Rautio,[1,2,3] Kirsten S. Christoffersen,[4,5] Laura Forsström,[6] Isabelle Laurion,[2,3,7] Heather L. Mariash,[8] Sari Peura,[9] Warwick F. Vincent[2,10]

[1]Département des Sciences Fondamentales, Université du Québec à Chicoutimi, Chicoutimi, Quebec, Canada; [2]Centre d'Études Nordiques (CEN), Université Laval, Quebec City, Quebec, Canada; [3]Group for Interuniversity Research in Limnology and Aquatic Environment (GRIL), Université de Montréal, Montreal, Quebec, Canada; [4]Freshwater Biological Laboratory, Department of Biology, University of Copenhagen, Copenhagen, Denmark; [5]Department of Arctic Biology, University Centre in Svalbard, Longyearbyen, Norway; [6]Department of Environmental Sciences, University of Helsinki, Helsinki, Finland; [7]Centre Eau Terre Environnement, Institut National de la Recherche Scientifique, Quebec City, Quebec, Canada; [8]Wildlife Research Division, Environment and Climate Change Canada, Ottawa, Ontario, Canada; [9]Department of Forest Mycology and Plant Pathology, Science for Life Laboratories, Swedish University of Agricultural Sciences, Uppsala, Sweden; [10]Département de Biologie, Université Laval, Quebec City, Quebec, Canada

Scientific Significance Statement

Frozen tundra soils are one of the largest pools of organic carbon in the Earth system. Climate warming and associated permafrost thawing have increased the risk that a large fraction of this carbon will be released to the atmosphere as greenhouse gases, particularly in the form of methane produced by the many aquatic ecosystems present throughout the subarctic and arctic regions. However, the changes induced in the carbon pool of northern waterbodies by these increasing terrigenous inputs have been little studied. Our synthesis of data for ponds at diverse locations across the circumpolar North reveals the strong influence of thawing permafrost on northern freshwaters, with a shift toward increasing dominance by land-derived organic carbon that may alter metabolic pathways and aquatic food webs.

Abstract

Climate change and permafrost thaw are unlocking the vast storage of organic carbon held in northern frozen soils. Here, we evaluated the effects of thawing ice-rich permafrost on dissolved organic matter (DOM) in freshwaters by optical analysis of 253 ponds across the circumpolar North. For a subset of waters in subarctic Quebec, we also quantified the contribution of terrestrial sources to the DOM pool by stable isotopes. The optical measurements showed a higher proportion of terrestrial carbon and a lower algal contribution to

*Correspondence: maximewauthy@hotmail.com

This article is part of the Special Issue: Carbon cycling in inland waters
Edited by: Emily Stanley and Paul del Giorgio

DOM in waters affected by thawing permafrost. DOM composition was largely dominated (mean of 93%) by terrestrial substances at sites influenced by thawing permafrost, while the terrestrial influence was much less in waterbodies located on bedrock (36%) or with tundra soils unaffected by thermokarst processes (42%) in the catchment. Our results demonstrate a strong terrestrial imprint on freshwater ecosystems in degrading ice-rich permafrost catchments, and the likely shift toward increasing dominance of land-derived organic carbon in waters with ongoing permafrost thaw.

Northern permafrost regions contain one of the largest pools of carbon in the Earth system (Schuur et al. 2015), and increased attention is now focused on how these massive carbon stocks may be mobilized and converted to greenhouse gases with ongoing climate change. One trajectory for this conversion is via microbial metabolism in the lakes and ponds that receive dissolved and particulate organic carbon from eroding permafrost soils. Many of these waterbodies are created by thermokarst (erosion and collapse of ice-rich permafrost), resulting in thaw or thermokarst lakes and ponds (Vonk et al. 2015), hereafter referred to as thaw ponds. In some parts of the Arctic landscape, these ponds are disappearing by drainage, evaporation, or infilling, while in other northern regions they are becoming larger and more numerous (Vincent et al. 2017). These waters represent one of the most abundant freshwater ecosystem types in northern regions, and collectively they have an estimated total surface area in the range 250,000–380,000 km^2 (Grosse et al. 2013); this accounts for approximately 25% of the estimated total area covered by lakes and ponds in the Arctic (1.4×10^6 km^2; Muster et al. 2017). They encompass a variety of transparencies and trophic conditions, and are likely to become more turbid and heterotrophic with increasing carbon inputs from thawing permafrost soils (Vonk et al. 2015). Thaw ponds are also known to be hotspots in the landscape for strong emissions of greenhouse gases to the atmosphere (Abnizova et al. 2012; Negandhi et al. 2013; Sepulveda-Jauregui et al. 2015; Matveev et al. 2016).

Although the effect of increasing export of terrestrial organic compounds from the catchment and shifts in aquatic metabolism are known to change the carbon pool composition and the proportion of carbon of terrestrial origin (which we refer to as allochthony) in temperate freshwaters (Solomon et al. 2015), little is known about these effects in circumpolar ponds, despite the abundance of these ecosystems across the northern landscape (Muster et al. 2017) and their key role in carbon cycling (Abnizova et al. 2012). In this study, we investigated the impact of permafrost thaw on the concentration and composition of dissolved organic matter (DOM) using a suite of chemical, biological, optical, and stable isotopic (δ^{13}C and δ^2H) measurements. We hypothesized that DOM concentrations are higher in ponds that have emerged due to thawing permafrost soils than in waterbodies not affected by thermokarst processes. We further hypothesized that terrestrial carbon compounds are most abundant in ponds draining thawing soils, while ponds in regions with rock outcrops and nondegrading permafrost soils are relatively more enriched in autochthonous DOM, the fraction originating from aquatic primary production. Specifically, we predicted that these relative proportions of terrestrial matter in the DOM pool of different pond types are expressed in the DOM δ^{13}C and δ^2H isotopic composition.

Methods

Study regions

During the summer periods from 2002 to 2016, we sampled a total of 253 ponds distributed in 14 circumpolar regions (Fig. 1), for a total of 356 samples, including from a subset of ponds (55) that were sampled more than one time during the 15 yr. The regions span over a wide geographic area, covering around 200 degrees of longitude (from Alaska to Russia) and 30 degrees of latitude (from Subarctic to High Arctic), and encompassing a large range of temperatures (mean annual from −2.6°C to −18°C), vegetation types (from spruce or birch forest and shrub tundra to polar desert), and permafrost cover (from sporadic to continuous coverage; further details in Supporting Information Table S1). We divided the ponds into three categories according to their catchment characteristics and exposure to permafrost thaw, following Rautio et al. (2011): (1) bedrock ponds (21 ponds), characterized by rocky surroundings and with little terrestrial vegetation, and no effect of thawing permafrost soils; (2) tundra ponds (88 ponds), not directly formed or significantly impacted by degrading permafrost soils, but surrounded by grass-, shrub-, or forest-tundra vegetation; and (3) thaw ponds (144 ponds), which are thermokarst waterbodies formed by thawing and collapse of ice-rich permafrost (Vonk et al. 2015). Photographs of the ponds in each category are shown in Supporting Information Fig. S1. The sampled ponds were smaller than 10 ha, with the exception of 17 larger but shallow (< 3.5 m) waterbodies.

Chemical and biological analyses

We collected surface-water samples to measure pH, total phosphorus (TP), total nitrogen (TN), and total dissolved iron (Fe) concentrations, and filtered subsamples through pre-rinsed cellulose acetate filters (0.2 μm) in order to analyze dissolved organic carbon (DOC) concentrations and perform optical analyses on the chromophoric DOM (CDOM; see below). This filter pore size removes small-size inorganic soil particles common in thaw ponds (Watanabe et al. 2011), and was chosen to be consistent with earlier studies on circumpolar ponds (Breton et al.
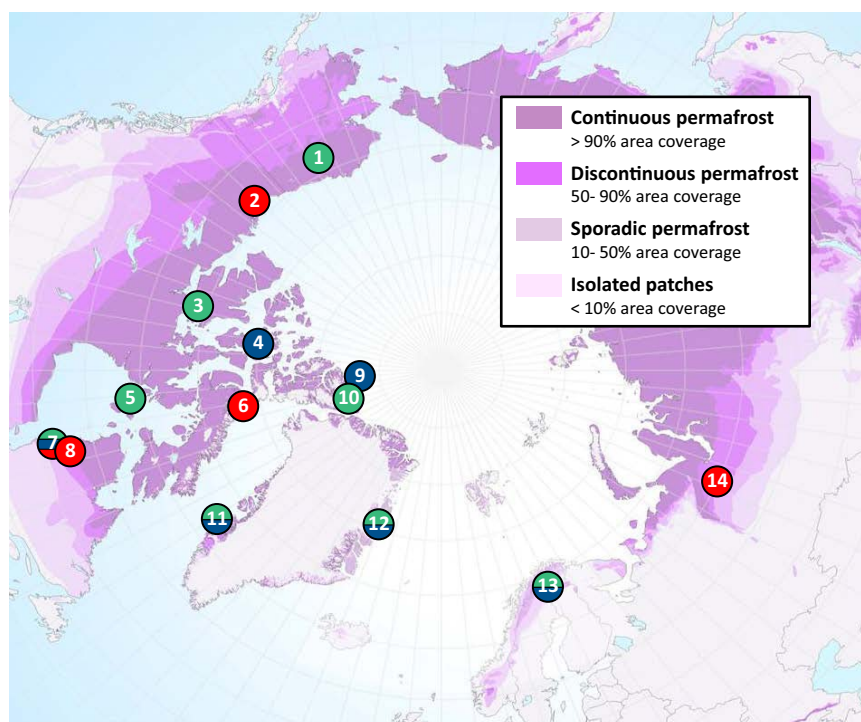
Fig. 1. Location of the 14 regions sampled in the north circumpolar permafrost zone. Circle colors indicate the types of ponds in the region: *blue* for bedrock, *green* for tundra, and *red* for thaw. 1 = Toolik, 2 = Mackenzie Delta, 3 = Cambridge Bay, 4 = Resolute Bay, 5 = Coral Harbor, 6 = Bylot Island, 7 = Kuujjuarapik, 8 = Umiujaq, 9 = Ward Hunt, 10 = Hazen, 11 = Kangerlussuaq, 12 = Zackenberg, 13 = Kilpisjärvi, 14 = Seida. Source of the permafrost map: Brown et al. (1998).

2009; Laurion et al. 2010; Roiha et al. 2015). The samples were stored in acid-washed and combusted glass vials at 4°C in the dark, and DOC quantification was carried out using a carbon analyzer (TOC-5000A or TOC-VCPH, Shimadzu, Kyoto, Japan). Seston in the surface water was filtered onto GF/F glass fiber filters to determine phytoplankton chlorophyll *a* (Chl *a*) concentrations, as in Nusch (1980).

Optical analyses

CDOM absorbance was measured between 250 nm and 800 nm using a UV-visible Cary 100 (Agilent, Santa Clara, California), Cary 300 (Agilent, Santa Clara, California), or LAMBDA 650 (PerkinElmer, Waltham, Massachusetts) spectrophotometer, depending on sample origin. After subtracting the blank spectrum, we applied a null-point adjustment, using the mean value from 750 nm to 800 nm, and report CDOM as the absorption coefficient at 320 nm (a_{320}) and 440 nm (a_{440}) according to the equation:

$$a_\lambda = 2.303 \times A_\lambda / L, \qquad (1)$$

where a_λ is the absorption coefficient (m^{-1}) at wavelength λ, A_λ the absorbance corrected at wavelength λ, and L the path length of the cuvette (m) (Blough and Del Vecchio 2002). The specific ultraviolet absorbance at 254 nm (SUVA$_{254}$) was determined from DOC normalized A_{254} as an index of

aromaticity and the relative proportion of terrestrial vs. algal carbon sources in DOM (Weishaar et al. 2003). Iron can complex humic substances and increase DOM absorbance in elevated concentrations, inducing an overestimation of SUVA$_{254}$ (Xiao et al. 2013), and we therefore applied the following equation when the Fe concentration was higher than 2 mg L^{-1} (Poulin et al. 2014):

$$A_{254 \text{ corrected}} = A_{254 \text{ measured}} - (0.0653 \times [\text{Fe}]) \qquad (2)$$

The Fe concentration was only higher than 2 mg L^{-1} in some ponds of Bylot Island (region 6), but this variable was not available for the regions of Zackenberg (region 12) and Seida (region 14). Therefore, the interpretation of the optical indices should be made with caution, especially in systems influenced by active permafrost erosion and containing high iron concentrations. We also determined spectral slopes (S) following Loiselle et al. (2009) for the intervals 279–299 (S_{289}, named by center wavelength), 275–295 (S_{285}) and 350–400 nm (S_{375}), and performed the regression calculations using SciLab v. 5.5.2. (Scilab Enterprises 2015). We used S_{289} to estimate the importance of fulvic and humic acids related to algal production (Loiselle et al. 2009), and the slope ratio (S_R) S_{285}/S_{375} was calculated as an index of CDOM molecular weight (Helms et al. 2008).

For a subsample of 100 ponds, we also recorded fluorescence intensity on a Cary Eclipse spectrofluorometer (Agilent,

Santa Clara, California) across the excitation waveband from 250 nm to 450 nm (10 nm increments) and emission waveband of 300–560 nm (2 nm increments) in order to construct excitation-emission matrices (EEMs). We calculated the fluorescence index (FI) as the ratio of fluorescence emission intensities at 450 nm and 500 nm at the excitation wavelength of 370 nm to investigate the origin of fulvic acids (McKnight et al. 2001). To identify and quantify the main DOM components, we ran a parallel factor (PARAFAC) model on 129 samples from 95 ponds in MATLAB v R2013a (MathWorks, Natick, Massachusetts), as in Murphy et al. (2013). We corrected EEMs for Raman and Rayleigh scattering and inner filter effects, and standardized the fluorescence to Raman units using the FDOMcorr 1.4 toolbox (Murphy et al. 2010). The model was performed on corrected EEMs and validated by split-half analysis (Supporting Information Fig. S2) using the drEEM toolbox from Murphy et al. (2013). For each sample, we summed the maximum fluorescence [Cx] of the different components x to determine the total fluorescence (F_T) and calculated the relative abundance of any component x, according to the following equation:

$$\%Cx = ([Cx]/F_T) \times 100 \qquad (3)$$

To identify the components of the model, we compared the excitation and emission spectra to published components from more than 70 papers available in the OpenFluor database, following Murphy et al. (2014).

Stable isotope analyses

To quantify the relative contribution of terrestrial carbon among pond types, we carried out stable isotope analyses (SIA) on surface-water DOM and its potential sources in a subsample of 10 ponds in the vicinity of Kuujjuarapik, subarctic Quebec (region 7 in Fig. 1). Given the presence of the three pond types in this same region sharing similar environmental conditions, Kuujjuarapik was a convenient place to perform such analyses. In addition to collecting soils surrounding ponds, DOM, benthic bulk material and seston were sampled in bedrock and tundra waterbodies for δ^{13}C and δ^2H analyses. Thaw ponds in Kuujjuarapik are located in a peatland with abundant semi-aquatic macrophytes. Because of their high turbidity, no light reaches the bottom in these ponds (as measured with an underwater radiometer; Li-Cor BioSciences, Lincoln, Nebraska), and strong thermal stratification limits the exchange between bottom and surface waters (Matveev et al. 2016). Therefore, we considered the contribution of benthic material to surface-water DOM to be negligible and took the wetland macrophytes into account as a potential source to DOM in these thaw ponds. DOM samples for stable isotopes were collected and stored as indicated in "Chemical and biological analyses" section. Soil samples were collected from the top layer (0–5 cm) close to the ponds. For bedrock and tundra ponds, this layer represents the shallow soils around the ponds, while for the thaw

ponds, this was surface soils from the organic-rich palsas that are collapsing into the ponds (*see* Fig. 7 in Vincent et al. 2017). In order to remove the carbonate, we applied an acid fumigation to the soil samples during 96 h prior the δ^{13}C analyses, as described in Ramnarine et al. (2011). Decaying submerged macrophytes (*Carex* sp.) were sampled from the edge of thaw ponds. In bedrock and tundra ponds, we sampled the surface of submerged rocks by scraping with a spatula to collect the epibenthic material. All samples were freeze-dried before SIA. DOM samples were analyzed for δ^{13}C using an Aurora 1030W TOC Analyzer (O.I. Corporation, College Station, Texas) coupled to a Finnigan DELTA plus Advantage MS (Thermo Fisher Scientific, Waltham, Massachusetts) in the G.G. Hatch Stable Isotope Laboratory (University of Ottawa, Ontario). The δ^{13}C analyses on soil and macrophyte samples were carried out using a FLASH 2000 OEA interfaced with a Delta V Plus MS (Thermo Fisher Scientific, Waltham, Massachusetts) in the RIVE Research Center (Université du Québec à Trois-Rivières, Quebec). All δ^2H analyses were performed in the Colorado Plateau Stable Isotope Laboratory (Northern Arizona University, Arizona) as in Doucett et al. (2007), using a CONFLO II coupled to a Delta Plus XL MS (Thermo Fisher Scientific, Waltham, Massachusetts). To determine the phytoplankton δ^{13}C signature, we used specific algal fatty acids (FAs) extracted from bulk seston as a proxy, performing SIA on 16:1n7, 18:2n6, 18:3n3, and 20:5n3 fractions (Taipale et al. 2015; Grosbois et al. 2017*a,b*). The FAs were transmethylated according to a protocol adapted from Lepage and Roy (1984). The δ^{13}C analyses on FAs were carried out in the Stable Isotope Laboratory of Memorial University (Memorial University of Newfoundland, Newfoundland and Labrador), using a 6890N GS (Agilent, Santa Clara, California) linked to a Delta V Plus MS (Thermo Fisher Scientific, Waltham, Massachusetts). We estimated the phytoplankton δ^2H signature from filtered water as in Grosbois et al. (2017*a*). As for the phytoplankton, we extracted the FAs from the benthic bulk material and performed δ^{13}C analyses on the 14:0, 16:0, and 18:0 fractions, which are saturated FAs specific to most organisms (Napolitano 1999), and were thus considered representative of the δ^{13}C isotopic composition of the benthic organic matter.

Mixing model

We considered three potential sources contributing to DOM in each pond type: soils, phytoplankton, and benthic bulk for bedrock and tundra ponds, and soils, phytoplankton, and macrophytes for thaw ponds. We performed a dual Bayesian mixing model adapted from Wilkinson et al. (2014), using δ^{13}C and δ^2H as end-members. The model was run in R v 3.3.2. (R Development Core Team 2016).

Statistical analyses

To determine how the chemical, biological, and optical properties were individually influenced by permafrost thaw, the data were analyzed by Kruskal-Wallis rank tests, with

pair-wise comparisons using a post hoc test (Bonferroni). We carried out principal component analyses (PCAs) and permutational multivariate analyses of variance (PERMANOVAs) on $\log_{10}(x + 1)$-transformed data to illustrate and test the influence of pond type on optical properties. The data were centered and standardized before applying the PCAs. In the PERMANOVAs, Euclidean distance was used as the dissimilarity index, and the number of permutations was fixed at 999. Pair-wise comparisons were performed using Bonferroni correction to identify differences among the types of ponds. The multivariate homogeneity of group dispersions was verified by performing a permutational analysis of multivariate dispersions (PERMDISP). All statistical analyses were performed on R v 3.3.2. (R Development Core Team 2016). The data from the 55 ponds that were sampled more than once but in different years were considered independent based on the assumption that in these rapidly changing landscapes, the biological, chemical, and optical properties of the ponds can vary greatly from one sampling year to another.

Results

Chemical, biological, and optical properties

The overall data set (archived in Wauthy et al. 2017) showed a strong effect of permafrost thaw (Fig. 2), with highly significant differences between thaw and non-thaw ponds for all variables, except for pH and %C4 ($p < 0.01$, Kruskal-Wallis by rank test). Chl *a*, TP, and TN had highest values in thaw ponds, indicating a more enriched trophic state. There were wide variations in DOC concentration, from 1.0 mg L^{-1} to 116.8 mg L^{-1}, with highest values in the thaw ponds. CDOM followed the same trend, as indicated by a_{320} and a_{440} values. SUVA$_{254}$ was also higher in thaw ponds, suggesting a larger proportion of terrestrial DOM in these ponds as compared to bedrock and tundra ponds. Consistent with this interpretation, S_{289}, S_R, and FI values were lowest in thaw ponds, suggesting smaller amounts of carbon derived from aquatic primary production, higher DOM molecular weights, and a terrestrial origin for fulvic acids, respectively.

The PARAFAC model identified five fluorescence components (Supporting Information Fig. S3), of which four shared fluorescence characteristics with humic materials from terrestrial (C1–C3) and microbial origin (C4). The last component (C5) presented spectra similar to amino acids or proteins, and was attributed to algal production (Stedmon and Markager 2005) (more details in Supporting Information Table S2). The percentage of terrestrial humic components (%C1–%C3) showed different patterns among the pond types (Fig. 2): while %C1 and %C2 were significantly higher in thaw ponds, %C3 was greater in the ponds not affected by permafrost thaw. Although terrestrial humic components dominated in all pond types, thaw ponds showed higher proportions of C1–C3 ($73.2\% \pm 10.2\%$) than bedrock

($63.4\% \pm 19.7\%$) and tundra ponds ($64.9\% \pm 15.5\%$). Moreover, thaw ponds had the highest mean value for %C4 ($17.6\% \pm 5.1\%$), further indicating the presence of humic-dominated microbial material in these ponds. However, the proportion was not different from bedrock ponds ($16.6\% \pm 5.6\%$). Finally, the proportion of DOM associated with algal production was small in the thaw ponds, as indicated by its significantly lower %C5 ($9.2\% \pm 7.0\%$).

The two PCAs showed the tendency of pond types to group according to optical properties (Fig. 3). Figure 3A is for the PCA performed on the subsample of 95 ponds for which we had both spectrophotometric and fluorometric properties; the first two components explained 74.8% of the total variability (PC1 52.4% and PC2 22.4%). We observed a significant effect of catchment type (PERMANOVA, $F_{2,126} = 19.1$, $p = 0.001$), with the three pond types forming three distinct clusters. However, only the thaw pond cluster was significantly different from the bedrock and tundra groups (pair-wise PERMANOVA comparisons, *p*-adjusted < 0.05). We applied the second PCA on the complete dataset, but only for DOC and DOM spectrophotometric proxies; the first two components explained 89.0% of the variance (PC1 72.6% and PC2 16.4%) (Fig. 3B). The effect of catchment type was again significant (PERMANOVA, $F_{2,353} = 65.52$, $p = 0.001$) and the three pond types formed three significantly different clusters (pair-wise PERMANOVA comparisons, *p*-adjusted < 0.05). Bedrock and tundra ponds were mainly defined by their positive correlation with S_R, S_{289}, and %C5, but were also positively correlated to FI, %C3, and [C5]. On the other hand, the thaw pond clustering was mostly defined by positive correlation with fluorescence components [C1], [C2], %C1, and %C2, and by CDOM (a_{320} and a_{440}), with further positive correlations with [C4], DOC, SUVA$_{254}$.

Source contributions to DOM

The isotopic signatures of DOM showed similar δ^{13}C values between the different pond types in the Kuujjuarapik region, within the range -29.5‰ to -27.3‰ (Fig. 4). However, the DOM deuterium signature δ^2H was more depleted in thaw ponds (-153.9 ± 11.0‰) compared to other ponds (-131.2 ± 8.2‰). Similarly, the phytoplankton δ^{13}C signature was more negative in thaw ponds than in non-thaw ponds (-37.1 ± 2.5‰ vs. -30.5 ± 0.8‰). According to its location in biplots (Fig. 4A,B), DOM in bedrock and tundra ponds fitted well within the polygon of source end-members, and appeared to be mainly composed of benthic and terrestrial materials. The DOM in thaw ponds was positioned at the limit of the polygon, with closest affinity to terrestrial sources (Fig. 4C).

The mixing model showed a large contribution of benthic (median of 55%) and terrestrial (median of 22%) material to the DOM of bedrock ponds, although the range of the 95% highest contribution probability showed high variabilities (0–97% and 0–99%, respectively) (Fig. 5A). The terrestrial sources were more substantial in tundra ponds (median of 42%), but the benthic material remained the principal
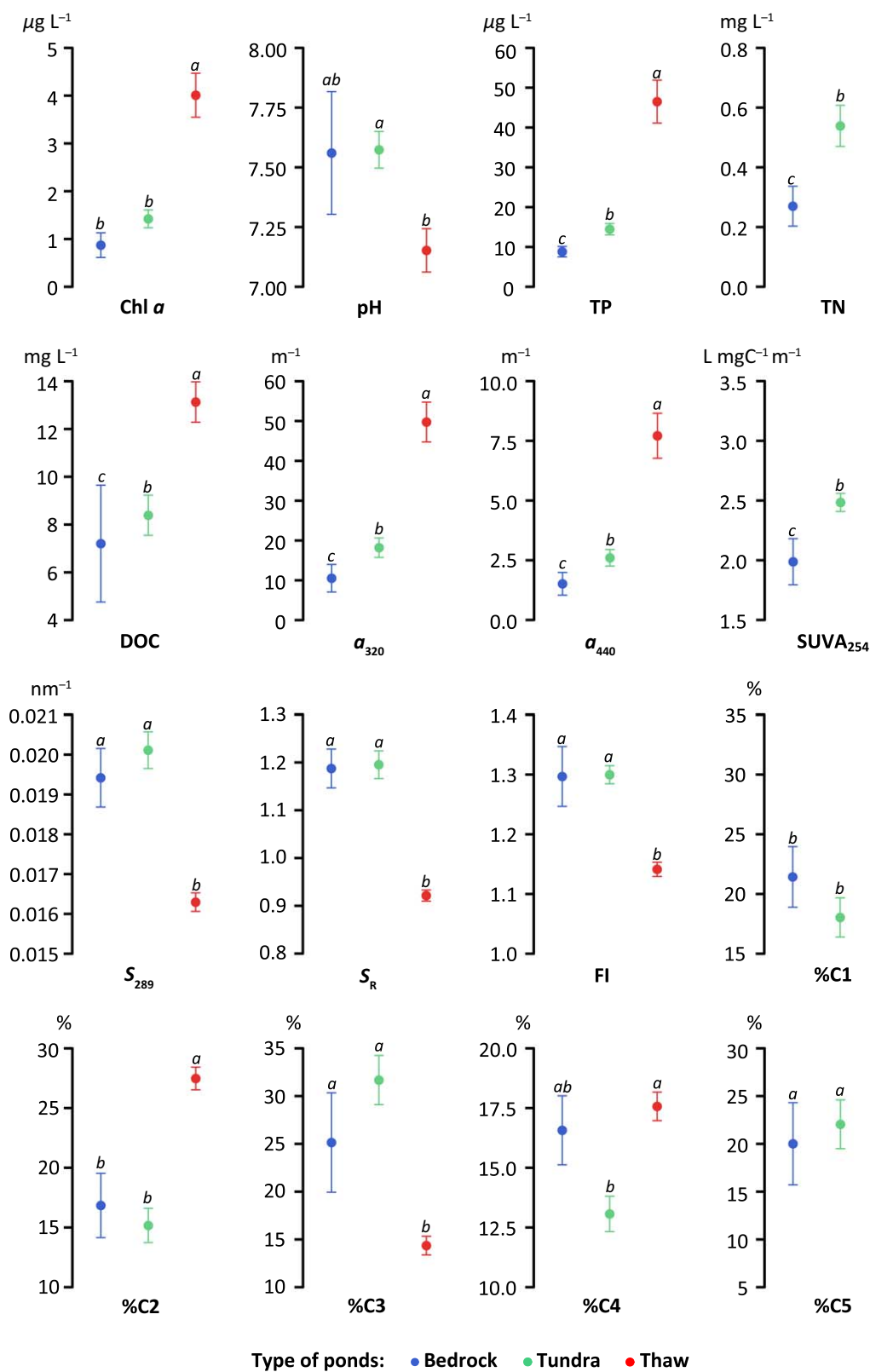
Fig. 2. Scatter plots of the mean ($+$ SE) values for biological, chemical, and optical variables in the different pond types. Abbreviations are defined in the text. Different letters above error bars indicate significant differences between ponds types ($p < 0.05$, Bonferroni post hoc test).
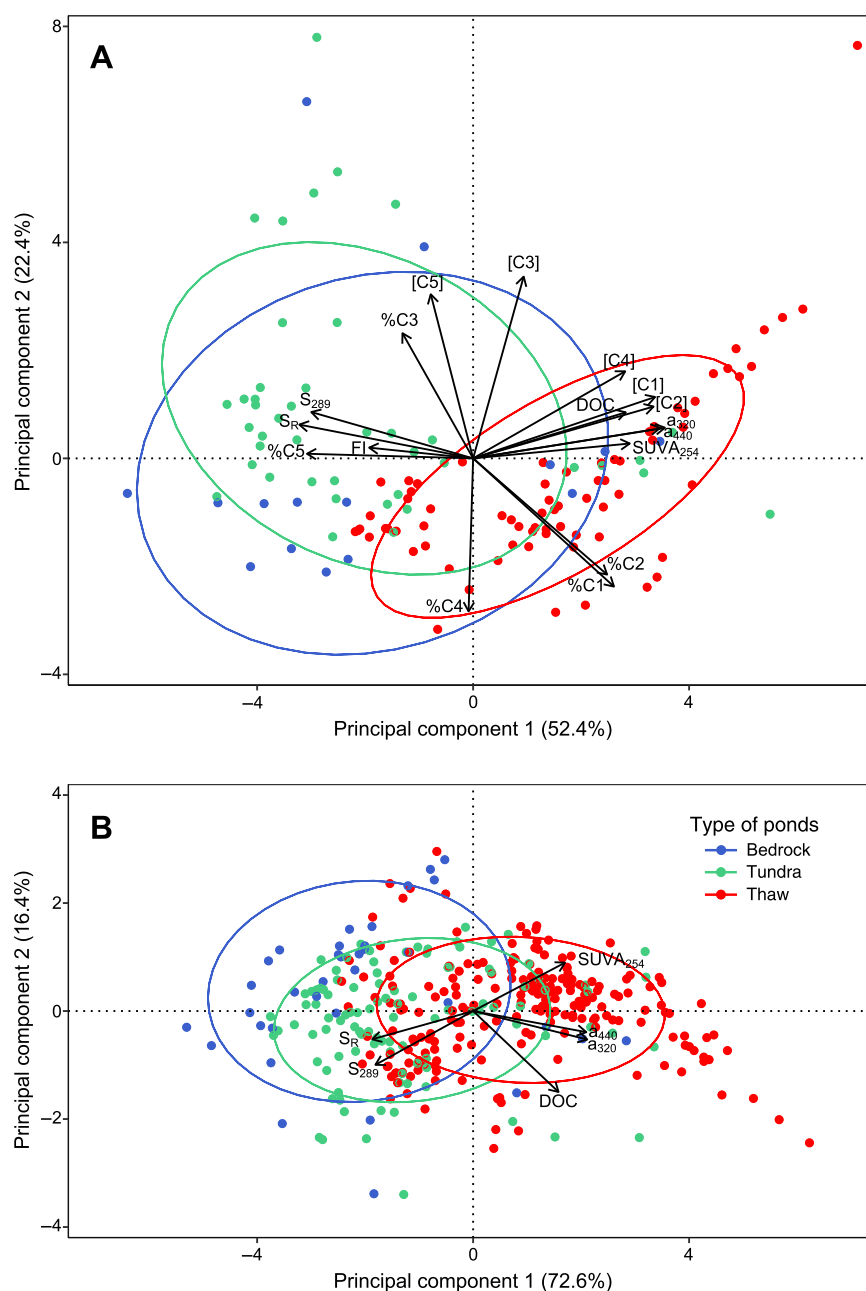
Fig. 3. PCAs of DOM optical variables across bedrock, tundra, and thaw ponds, for spectral and fluorescence indices, and PARAFAC components in 95 ponds (**A**), and for only spectrophotometric indices, including all 253 ponds (**B**). Arrows indicate the loadings of the different variables. Ellipses group each pond type (ellipse probability = 0.68). Abbreviations are defined in the text.

contributor to DOM (median of 47%) (Fig. 5B). However, the range was also high for the two main sources (2–90% for the benthic source, and 2–82% for the terrestrial source). Phytoplankton was a significant but minor source of DOM in both pond types not affected by thawing permafrost, with a median of 11% and 6% in bedrock and tundra ponds, respectively. In the thaw ponds, there was a major shift to a higher proportion of carbon from terrestrial origin for DOM, with terrestrial sources contributing 96% (median, Fig. 5C)

and negligible contributions from phytoplankton and macrophytes (medians less than 2%).

Discussion

Nutrients and primary producers

The studied 253 ponds spanned a wide gradient of environmental conditions, from transparent oligotrophic waterbodies in areas not affected by thawing permafrost, to humic- and
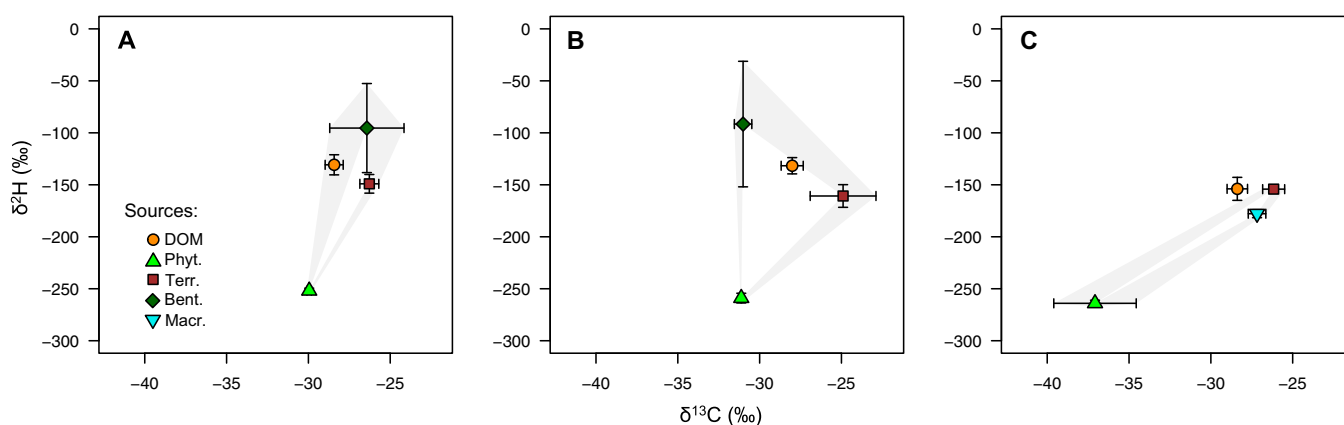
Fig. 4. Distribution of δ^{13}C and δ^2H DOM signatures inside a polygon of the potential sources (+ SD) in Kuujjuarapik ponds (region 7) with (**A**) bedrock catchment, (**B**) tundra catchment unaffected by thermokarstic processes, and (**C**) thawing permafrost catchment. The sources are phytoplankton (Phyt.), terrestrial organic matter (Terr.), benthic organic matter (Bent.), and macrophytes (Macr.).
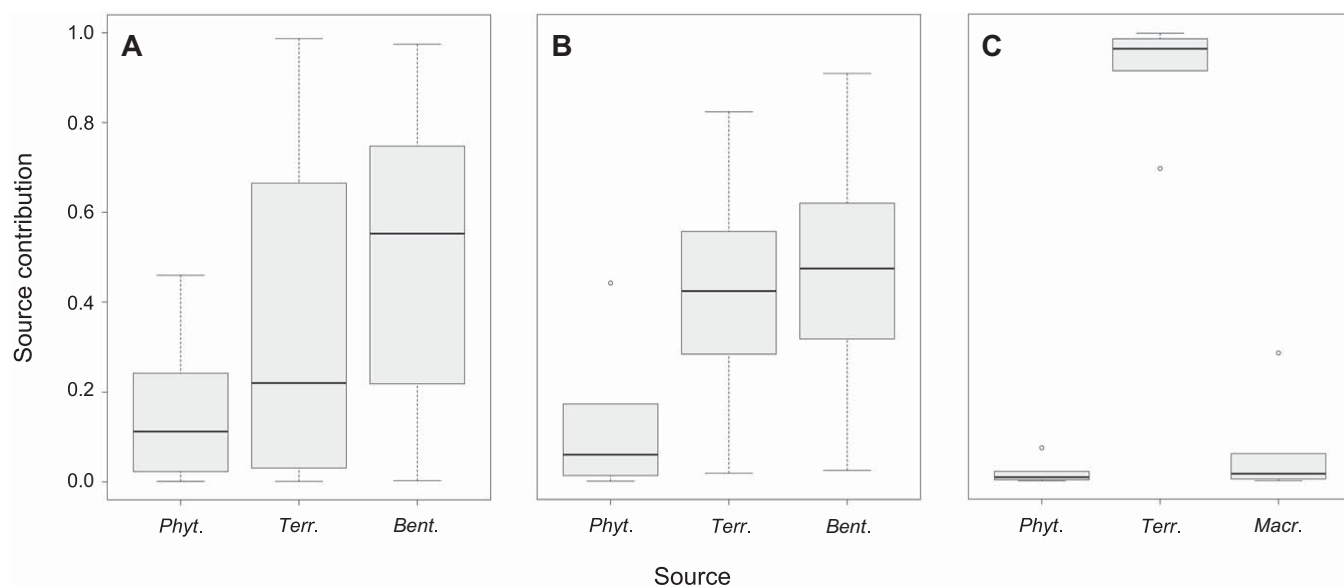

Fig. 5. Source contributions to DOM in Kuujjuarapik ponds (region 7) with (**A**) bedrock catchment, (**B**) tundra catchment unaffected by thermokarstic processes, and (**C**) thawing permafrost catchment, based on a dual isotope (δ^{13}C and δ^2H) Bayesian mixing model. The sources are phytoplankton (Phyt.), terrestrial organic matter (Terr.), benthic organic matter (Bent.), and macrophytes (Macr.). Whiskers and boxes show the distribution of 95% and 50% highest densities of contribution probabilities, respectively, with the median value indicated by the line within each box.

nutrient-rich ponds exposed to thermal erosion (Fig. 2). Nutrients in bedrock and tundra ponds were typical of oligotrophic freshwater systems, and comparable to values usually found in clear-water high-latitude ponds (Rautio et al. 2011). In thaw ponds, they showed values more characteristic of mesotrophic and eutrophic systems, and likely originated from the eroding catchment (Larsen et al. 2017). Following the low nutrient concentrations in the water column, Chl *a* values in bedrock and tundra ponds indicated low phytoplankton biomass. Consequently, most primary production in clear-water ponds is produced by the benthic mat and biofilm communities, with phytoplankton often representing less

than 2% of the total photosynthetic biomass in these systems (Bonilla et al. 2005; Rautio et al. 2011). In thaw ponds, more elevated Chl *a* values suggested a higher planktonic primary production, more probably supported by the higher nutrient concentrations (Vonk et al. 2015). However, the higher CDOM concentrations and suspended solids in thaw ponds efficiently attenuate the solar radiation (Watanabe et al. 2011), limiting benthic and therefore overall primary production (Vadeboncoeur et al. 2008). Increased terrestrial DOM in circumpolar surface waters could therefore lead to a considerable decrease in the light availability for photosynthesis, resulting in a shift toward a heterotrophic production-based food web

as has been documented in experimental conditions (Forsström et al. 2015), and a high production of CO_2 and CH_4 (Roiha et al. 2015).

DOC and CDOM properties

Highest DOC and CDOM values were observed in the thaw ponds, with several CDOM proxies indicating higher terrestrial inputs from the catchment (Fig. 2). Similar accumulation of DOM has also been reported previously at circumpolar sites with high terrestrial inputs (Vonk et al. 2013; Abbott et al. 2014; Roiha et al. 2015). The elevated values of a_{320} and a_{440} in thaw ponds indicate high concentrations of CDOM, inducing more light attenuation in the water column. Consistent with earlier studies, S_R, S_{289}, and $SUVA_{254}$ indicated fresher aromatic compounds of higher molecular weight and a large proportion of terrestrial vs. algal carbon sources in thaw ponds (e.g., Roiha et al. 2015). This high degree of DOM allochthony in thaw ponds was also supported by low values of FI, an indicator of large inputs of fulvic acids from terrestrial sources and a function of carbon storage in the catchment (Rantala et al. 2016).

The association of [C1] and [C2] with $SUVA_{254}$ and other CDOM proxies in ponds influenced by thawing permafrost also indicates strong DOM allochthony in these waters (Fig. 3A), with high inputs of DOM from the catchment. C3 also had fluorescence characteristics of humic materials from a terrestrial origin, but showed an opposite association with C1 and C2. This suggests that C3 could be the product of biological transformation of C1 and C2 in the water column (Jørgensen et al. 2011). C4 matched well with humic materials of microbial origin, and therefore can be linked to the degradation of both algal and terrestrial sources. Finally, the amino acid- or protein-like algal component C5 showed higher values in bedrock and tundra ponds, and negative relationships with $SUVA_{254}$ and thawing permafrost, indicating a greater algal origin of DOM in non-thaw ponds. This algal signature likely reflects the benthic primary production in these ponds, given its dominant contribution to overall algal biomass in clear-water circumpolar ponds (Rautio et al. 2011).

It is important to note that we focused on thermokarst ponds, with permafrost thaw and degradation along pond banks, as is commonly found across the North. There are other modes of permafrost thaw that can have different consequences for surface-water DOM concentrations and composition. For instance, in certain hydrological conditions, catchment-scale permafrost thaw via active layer thickening or permafrost loss can reduce DOC concentrations or $SUVA_{254}$ values (Cory et al. 2013; O'Donnell et al. 2014). The highly variable organic carbon content of thawing permafrost soils (Vincent et al. 2017) may also influence the DOM properties in the receiving waterbodies. In this study, we did not measure the organic carbon content in the watershed, but the existing information from the study regions

(Bouchard et al. 2015; Vincent et al. 2017) as well as our observations of the bank morphology and benthic substrates indicate that the studied thaw ponds were predominantly located in organic-rich sites. Therefore, substantial impacts of permafrost thaw on pond DOM were expected.

Thawing of ice-rich permafrost appears to have a strong effect on the ratio of allochthonous to autochthonous DOM in surface waters, resulting from direct inputs of allochthonous DOM from eroding permafrost soils, and from its effect on DOM age (O'Donnell et al. 2014), in situ transformations and respiration (Laurion and Mladenov 2013; Cory et al. 2014). In particular, the level of bacterial and photochemical transformation of terrigenous DOM is likely to vary between the turbid and bacteria-rich thaw ponds as compared to clear and oligotrophic waters of non-thaw ponds, with important consequences on DOM allochthony. Moreover, drivers that are independent of permafrost thaw could potentially explain part of the differences observed between thaw and non-thaw ponds. These drivers include the composition, size and slopes of the catchment (Olefeldt et al. 2014; Vonk et al. 2015), influence of groundwater and precipitation (Olefeldt et al. 2013), water retention time (Catalán et al. 2016) and temperature (Porcal et al. 2015). However, our sampling covered a great variety of environments, mitigating the influence of these other factors as drivers of the observed DOM differences among pond types. Furthermore, although some of these other factors likely differed considerably between bedrock and tundra ponds, the overall water chemistry as well as the DOM concentrations and optical characteristics differed less between these two pond types than for the thaw ponds. Additionally, the DOM sourcing by stable isotope analysis for ponds in the Kuujjuarapik region indicated that these other drivers were less likely relative to allochthony. Overall, our results point to the importance of thawing permafrost for the biogeochemistry of circumpolar surface waters.

DOM contribution quantification

In the subarctic region of Kuujjuarapik (region 7), the SIA data and the mixing model supported the optical analyses and confirmed a high terrestrial DOM input in thaw ponds (Fig. 5). However, terrestrial sources were also important in non-thaw ponds, particularly in tundra ponds where soils and benthic material contributed equally to DOM. This proportional influence of terrestrial inputs likely reflects the limitation of autochthonous sources under oligotrophic nutrient conditions, as well as the large perimeter length per unit area of these small waterbodies that would favor interactions with the surrounding tundra soils.

The DOM contribution by phytoplankton was low in bedrock and tundra ponds of the region, as to be expected given the low algal biomass and primary production in the water column compared to the benthos in these ponds (Rautio and Vincent 2006), and supporting studies that have shown

a low contribution of phytoplankton to the food webs of circumpolar ponds (Cazzanelli et al. 2012; Mariash et al. 2014). In the thaw ponds, phytoplankton biomass was higher, possibly from more enriched nutrient conditions, but nevertheless its contribution to DOM was insignificant and overwhelmed by the terrestrial signal.

The δ^{13}C signatures of phytoplankton were more depleted in the thaw ponds vs. non-thaw ponds (Fig. 4), and an explanation of this may lie in their elevated concentrations of methane (Matveev et al. 2016). Due to the fractionation during methanogenesis, methane has more negative δ^{13}C values and can be metabolized by methanotrophic bacteria, which then enter the food web (Bastviken et al. 2003). Mixotrophic algae constitute a major fraction of the total phytoplankton community growing in the thaw ponds of the region (Bégin and Vincent 2017) and could rely on the methanotrophic bacteria as an energy source, explaining the more depleted δ^{13}C signature of the phytoplankton. Given the extreme shallowness (< 1 m) and the absence of stratification in bedrock and tundra ponds, the benthic source was an important contributor to DOM, likely resulting from the resuspension of decomposed benthic materials (Evans 1994) and by diffusion of benthic carbon exudates to the water column (Rautio et al. 2011; Rodríguez et al. 2013).

In the thaw ponds, the DOM isotopic signature was close to the outside of the polygon defined by our three selected sources (Fig. 4C). One explanation could be that we missed a source contributing to DOM. Since the studied thaw ponds are located in a peatland, mosses (*Sphagnum* spp.) are abundant in the catchment and could be a candidate for this missing source. However, we sampled *Sphagnum* mosses as a potential end-member, and found that their isotopic signature was similar to macrophytes (δ^{13}C of $-26.6\permil$ vs. $-27.2\permil$, δ^2H of $-180.9\permil$ vs. $-177.8\permil$); hence, *Sphagnum* effect was considered to be included in the macrophyte values in the mixing model. A more plausible explanation may be that labile, ^{13}C-enriched terrestrial matter is rapidly metabolized by bacteria once in the ponds, leaving the more depleted and recalcitrant fraction dissolved in the water column, and causing more negative δ^{13}C DOM values (Biasi et al. 2005; Bianchi and Canuel 2011).

Conclusions

Consistent with previous syntheses (Vonk et al. 2015; Wrona et al. 2016), our observations underscore the large variations in limnological properties among northern high-latitude waters. Despite this variability, there was a clear effect of permafrost thaw, resulting in more allochthony, higher DOC concentrations, and DOM with a predominantly land-derived signature. To our knowledge, this is the first time the DOM has been reported in this extent to waterbodies in the circumpolar North. The increasing terrestrial influence on arctic and subarctic ponds results in decreased water column transparency, which in turn will affect biogeochemical

processes, energy supply to benthic primary producers, and the balance of autochthonous and allochthonous production. These impacts may be viewed together as an example of "browning" that is being observed throughout the world with increasing concern (Graneli 2012; Williamson et al. 2015). Because of the erodible and DOM-rich nature of the permafrost landscape, northern browning is an extreme version of this global phenomenon, and may be compounded in the future by increased rainfall and extreme weather events (Vincent et al. 2017). This extreme browning will likely shift northern freshwaters more toward net heterotrophic conditions, increased DOM flocculation and oxygen depletion, and greater production of greenhouse gases across the circumpolar North.

References

Abbott, B. W., J. R. Larouche, J. B. Jones, W. B. Bowden, and A. W. Balser. 2014. Elevated dissolved organic carbon biodegradability from thawing and collapsing permafrost. J. Geophys. Res. Biogeosci. **119**: 2049–2063. doi:10.1002/2014JG002678

Abnizova, A., J. Siemens, M. Langer, and J. Boike. 2012. Small ponds with major impact: The relevance of ponds and lakes in permafrost landscapes to carbon dioxide emissions. Global Biogeochem. Cycles **26**: GB2041. doi:10.1029/2011GB004237

Bastviken, D., J. Ejlertsson, I. Sundh, and L. Tranvik. 2003. Methane as a source of carbon and energy for lake pelagic food webs. Ecology **84**: 969–981. doi:10.1890/0012-9658(2003)084[0969:MAASOC]2.0.CO;2]

Bégin, P. N., and W. F. Vincent. 2017. Permafrost thaw lakes and ponds as habitats for abundant rotifer populations. Arct. Sci. **3**: 354–377. doi:10.1139/as-2016-0017

Bianchi, T. S., and E. A. Canuel. 2011. Stable isotopes and radiocarbon, p. 30–48. *In* T. S. Bianchi and E. A. Canuel [eds.], Chemical biomarkers in aquatic ecosystems. Princeton Univ. Press.

Biasi, C., O. Rusalimova, H. Meyer, C. Kaiser, W. Wanek, P. Barsukov, H. Junger, and A. Richter. 2005. Temperature-dependent shift from labile to recalcitrant carbon sources of arctic heterotrophs. Rapid Commun. Mass Spectrom. **19**: 1401–1408. doi:10.1002/rcm.1911

Blough, N. V., and R. Del Vecchio. 2002. Chromophoric DOM in the coastal environment, p. 509–546. *In* D. A. Hansell and C. A. Carlson [eds.], Biogeochemistry of marine dissolved organic matter. Academic Press.

Bonilla, S., V. Villeneuve, and W. F. Vincent. 2005. Benthic and planktonic algal communities in a high Arctic Lake: Pigment structure and contrasting responses to nutrient enrichment. J. Phycol. **41**: 1120–1130. doi:10.1111/j.1529-8817.2005.00154.x

Bouchard, F., I. Laurion, V. Préskienis, D. Fortier, X. Xu, and M. J. Whiticar. 2015. Modern to millennium-old greenhouse gases emitted from ponds and lakes of the Eastern

Canadian Arctic (Bylot Island, Nunavut). Biogeosciences **12**: 7279–7298. doi:10.5194/bg-12-7279-2015

Breton, J., C. Vallières, and I. Laurion. 2009. Limnological properties of permafrost thaw ponds in northeastern Canada. Can. J. Fish. Aquat. Sci. **66**: 1635–1648. doi:10.1139/f09-108

Brown, J., O. J. Ferrians, J. A. Heginbottom, and E. S. Melnikov. 1998. Circum-arctic map of permafrost and ground ice conditions. National Snow and Ice Data Center.

Catalán, N., R. Marcé, D. N. Kothawala, and L. J. Tranvik. 2016. Organic carbon decomposition rates controlled by water retention time across inland waters. Nat. Geosci. **9**: 501–504. doi:10.1038/ngeo2720

Cazzanelli, M., L. Forsström, M. Rautio, A. Michelsen, and K. S. Christoffersen. 2012. Benthic resources are the key to *Daphnia middendorffiana* survival in a high arctic pond. Freshw. Biol. **57**: 541–551. doi:10.1111/j.1365-2427.2011.02722.x

Cory, R. M., B. C. Crump, J. A. Dobkowski, and G. W. Kling. 2013. Surface exposure to sunlight stimulates CO_2 release from permafrost soil carbon in the Arctic. Proc. Natl. Acad. Sci. USA **110**: 3429–3434. doi:10.1073/pnas.1214104110

Cory, R. M., C. P. Ward, B. C. Crump, and G. W. Kling. 2014. Sunlight controls water column processing of carbon in Arctic fresh waters. Science **345**: 925–928. doi:10.1126/science.1253119

Doucett, R. R., J. C. Marks, D. W. Blinn, M. Caron, and B. A. Hungate. 2007. Measuring terrestrial subsidies to aquatic food webs using stable isotopes of hydrogen. Ecology **88**: 1587–1592. doi:10.1890/06-1184

Evans, R. D. 1994. Empirical evidence of the importance of sediment resuspension in lakes. Hydrobiologia **284**: 5–12. doi:10.1007/BF00005727

Forsström, L., M. Rautio, M. Cusson, S. Sorvari, R. L. Albert, M. Kumagai, and A. Korhola. 2015. Dissolved organic matter concentration, optical parameters and attenuation of solar radiation in high-latitude lakes across three vegetation zones. Écoscience **22**: 17–31. doi:10.1080/11956860.2015.1047137

Graneli, W. 2012. Brownification of lakes, p. 117–119. *In* L. Bengtsson, R. W. Herschy, and R. W. Fairbridge [eds.], Encyclopedia of lakes and reservoirs. Springer.

Grosbois, G., P. A. del Giorgio, and M. Rautio. 2017*a*. Zooplankton allochthony is spatially heterogeneous in a boreal lake. Freshw. Biol. **62**: 474–490. doi:10.1111/fwb.12879

Grosbois, G., H. Mariash, T. Schneider, and M. Rautio. 2017*b*. Under-ice availability of phytoplankton lipids is key to freshwater zooplankton winter survival. Sci. Rep. **7**: 11543. doi:10.1038/s41598-017-10956-0

Grosse, G., B. Jones, and C. Arp. 2013. Thermokarst lakes, drainage, and drained basins, p. 325–353. *In* J. F. Shroder, R. Giardino, and J. Harbor [eds.], Treatise on geomorphology. Academic Press.

Helms, J. R., A. Stubbins, J. D. Ritchie, E. C. Minor, D. J. Kieber, and K. Mopper. 2008. Absorption spectral slopes and slope ratios as indicators of molecular weight, source, and photobleaching of chromophoric dissolved organic matter. Limnol. Oceanogr. **53**: 955–969. doi:10.4319/lo.2008.53.3.0955

Jørgensen, L., C. A. Stedmon, T. Kragh, S. Markager, M. Middelboe, and M. Søndergaard. 2011. Global trends in the fluorescence characteristics and distribution of marine dissolved organic matter. Mar. Chem. **126**: 139–148. doi:10.1016/j.marchem.2011.05.002

Larsen, A. S., J. A. O'Donnell, J. H. Schmidt, H. J. Kristenson, and D. K. Swanson. 2017. Physical and chemical characteristics of lakes across heterogeneous landscapes in arctic and subarctic Alaska. J. Geophys. Res. Biogeosci. **122**: 989–1008. doi:10.1002/2016JG003729

Laurion, I., W. F. Vincent, S. MacIntyre, L. Retamal, C. Dupont, P. Francus, and R. Pienitz. 2010. Variability in greenhouse gas emissions from permafrost thaw ponds. Limnol. Oceanogr. **55**: 115–133. doi:10.4319/lo.2010.55.1.0115

Laurion, I., and N. Mladenov. 2013. Dissolved organic matter photolysis in Canadian arctic thaw ponds. Environ. Res. Lett. **8**: 035026. doi:10.1088/1748-9326/8/3/035026

Lepage, G., and C. C. Roy. 1984. Improved recovery of fatty acid through direct transesterification without prior extraction or purification. J. Lipid Res. **25**: 1391–1396.

Loiselle, S. A., L. Bracchini, A. Cózar, A. M. Dattilo, A. Tognazzi, and C. Rossi. 2009. Variability in photobleaching yields and their related impacts on optical conditions in subtropical lakes. J. Photochem. Photobiol. B Biol. **95**: 129–137. doi:10.1016/j.jphotobiol.2009.02.002

Mariash, H. L., S. P. Devlin, L. Forsström, R. I. Jones, and M. Rautio. 2014. Benthic mats offer a potential subsidy to pelagic consumers in tundra pond food webs. Limnol. Oceanogr. **59**: 733–744. doi:10.4319/lo.2014.59.3.0733

Matveev, A., I. Laurion, B. N. Deshpande, N. Bhiry, and W. F. Vincent. 2016. High methane emissions from thermokarst lakes in subarctic peatlands. Limnol. Oceanogr. **61**: S150–S164. doi:10.1002/lno.10311

McKnight, D. M., E. W. Boyer, P. K. Westerhoff, P. T. Doran, T. Kulbe, and D. T. Andersen. 2001. Spectrofluorometric characterization of dissolved organic matter for indication of precursor organic material and aromaticity. Limnol. Oceanogr. **46**: 38–48. doi:10.4319/lo.2001.46.1.0038

Murphy, K. R., K. D. Butler, R. G. M. Spencer, C. A. Stedmon, J. R. Boehme, and G. R. Aiken. 2010. Measurement of dissolved organic matter fluorescence in aquatic environments: An interlaboratory comparison. Environ. Sci. Technol. **44**: 9405–9412. doi:10.1021/es102362t

Murphy, K. R., C. A. Stedmon, D. Graeber, and R. Bro. 2013. Fluorescence spectroscopy and multi-way techniques. PARAFAC. Anal. Methods **5**: 6557–6566. doi:10.1039/c3ay41160e

Murphy, K. R., C. A. Stedmon, P. Wenig, and R. Bro. 2014. OpenFluor- an online spectral library of auto-fluorescence by organic compounds in the environment. Anal. Methods **6**: 658–661. doi:10.1039/c3ay41935e

Muster, S., and others. 2017. PeRL: A circum-Arctic Permafrost Region Pond and Lake database. Earth Syst. Sci. Data **9**: 317–348. doi:10.5194/essd-9-317-2017

Napolitano, G. E. 1999. Fatty acids as trophic and chemical markers in freshwater ecosystems, p. 21–44. *In* M. T. Arts and B. C. Wainman [eds.], Lipids in freshwater ecosystems. Springer.

Negandhi, K., I. Laurion, M. J. Whiticar, P. E. Galand, X. Xu, C. Lovejoy, and V. Shah. 2013. Small thaw ponds: An unaccounted source of methane in the Canadian High Arctic. PLoS One **8**: e78204. doi:10.1371/journal.pone.0078204

Nusch, E. A. 1980. Comparison of different methods for chlorophyll and phaeopigments determination. Arch. Hydrobiol. **14**: 14–35.

O'Donnell, J. A., G. R. Aiken, M. A. Walvoord, P. A. Raymond, K. D. Butler, M. M. Dornblaser, and K. Heckman. 2014. Using dissolved organic matter age and composition to detect permafrost thaw in boreal watersheds of interior Alaska. J. Geophys. Res. Biogeosci. **119**: 2155–2170. doi:10.1002/2014JG002695

Olefeldt, D., N. Roulet, R. Giesler, and A. Persson. 2013. Total waterborne carbon export and DOC composition from ten nested subarctic peatland catchments—importance of peatland cover, groundwater influence, and inter-annual variability of precipitation patterns. Hydrol. Process. **27**: 2280–2294. doi:10.1002/hyp.9358

Olefeldt, D., A. Persson, and M. R. Turetsky. 2014. Influence of the permafrost boundary on dissolved organic matter characteristics in rivers within the Boreal and Taiga plains of western Canada. Environ. Res. Lett. **9**: 035005. doi:10.1088/1748-9326/9/3/035005

Porcal, P., P. J. Dillon, L. A. Molot, and A. Almeida. 2015. Temperature dependence of photodegradation of dissolved organic matter to dissolved inorganic carbon and particulate organic carbon. PLoS One **10**: e0128884. doi:10.1371/journal.pone.0128884

Poulin, B. A., J. N. Ryan, and G. R. Aiken. 2014. Effects of iron on optical properties of dissolved organic matter. Environ. Sci. Technol. **48**: 10098–10106. doi:10.1021/es502670r

R Development Core Team. 2016. R: A language and environment for statistical computing. R Foundation for Statistical Computing.

Ramnarine, R., R. P. Voroney, C. Wagner-Riddle, and K. E. Dunfield. 2011. Carbonate removal by acid fumigation for measuring the $\delta^{13}C$ of soil organic carbon. Can. J. Soil Sci. **91**: 247–250. doi:10.4141/CJSS10066

Rantala, M. V., L. Nevalainen, M. Rautio, A. Galkin, and T. P. Luoto. 2016. Sources and controls of organic carbon in lakes across the subarctic treeline. Biogeochemistry **129**: 235–253. doi:10.1007/s10533-016-0229-1

Rautio, M., and W. F. Vincent. 2006. Benthic and pelagic food resources for zooplankton in shallow high-latitude lakes and ponds. Freshw. Biol. **51**: 1038–1052. doi:10.1111/j.1365-2427.2006.01550.x

Rautio, M., F. Dufresne, I. Laurion, S. Bonilla, W. F. Vincent, and K. S. Christoffersen. 2011. Shallow freshwater ecosystems of the circumpolar Arctic. Écoscience **18**: 204–222. doi:10.2980/18-3-3463

Rodríguez, P., J. Ask, C. L. Hein, M. Jansson, and J. Karlsson. 2013. Benthic organic carbon release stimulates bacterioplankton production in a clear-water subarctic lake. Freshw. Sci. **32**: 176–182. doi:10.1899/12-005.1

Roiha, T., I. Laurion, and M. Rautio. 2015. Carbon dynamics in highly heterotrophic subarctic thaw ponds. Biogeosciences **12**: 7223–7237. doi:10.5194/bg-12-7223-2015

Schuur, E. A. G., and others. 2015. Climate change and the permafrost carbon feedback. Nature **520**: 171–179. doi:10.1038/nature14338

Scilab Enterprises. 2015. Scilab: Free and open source software for numerical computation (OS, version 5.5.2.). Scilab Enterprises.

Sepulveda-Jauregui, A., K. M. Walter Anthony, K. Martinez-Cruz, S. Greene, and F. Thalasso. 2015. Methane and carbon dioxide emissions from 40 lakes along a north–south latitudinal transect in Alaska. Biogeosciences **12**: 3197–3223. doi:10.5194/bg-12-3197-2015

Solomon, C. T., and others. 2015. Ecosystem consequences of changing inputs of terrestrial dissolved organic matter to lakes: Current knowledge and future challenges. Ecosystems **18**: 376–389. doi:10.1007/s10021-015-9848-y

Stedmon, C. A., and S. Markager. 2005. Resolving the variability in dissolved organic matter fluorescence in a temperate estuary and its catchment using PARAFAC analysis. Limnol. Oceanogr. **50**: 686–697. doi:10.4319/lo.2005.50.2.0686

Taipale, S. J., E. Peltomaa, M. Hiltunen, R. I. Jones, M. W. Hahn, C. Biasi, and M. T. Brett. 2015. Inferring phytoplankton, terrestrial plant and bacteria bulk $\delta^{13}C$ values from compound specific analyses of lipids and fatty acids. PLoS One **10**: e0133974. doi:10.1371/journal.pone.0133974

Vadeboncoeur, Y., G. Peterson, M. J. Vander Zanden, and J. Kalff. 2008. Benthic algal production across lake size gradients: Interactions among morphometry, nutrients, and light. Ecology **89**: 2542–2552. doi:10.1890/07-1058.1

Vincent, W. F., M. Lemay, and M. Allard. 2017. Arctic permafrost landscapes in transition: Towards an integrated Earth system approach. Arct. Sci. **3**: 39–64. doi:10.1139/as-2016-0027

Vonk, J. E., and others. 2013. High biolability of ancient permafrost carbon upon thaw. Geophys. Res. Lett. **40**: 2689–2693. doi:10.1002/grl.50348

Vonk, J. E., and others. 2015. Reviews and syntheses: Effects of permafrost thaw on Arctic aquatic ecosystems. Biogeosciences **12**: 7129–7167. doi:10.5194/bg-12-7129-2015

Watanabe, S., I. Laurion, K. Chokmani, R. Pienitz, and W. F. Vincent. 2011. Optical diversity of thaw ponds in discontinuous permafrost: A model system for water color

analysis. J. Geophys. Res. **116**: G02003. doi:10.1029/2010JG001380

Wauthy, M., and others. 2017. Dissolved organic carbon and related environmental data from ponds and lakes in the circumpolar North, v. 1.0 (2002–2016). Nordicana **D31**. doi:10.5885/45520CE-0A48ADE0E2194290

Weishaar, J. L., G. R. Aiken, B. A. Bergamaschi, M. S. Fram, R. Fuji, and K. Mopper. 2003. Evaluation of specific ultraviolet absorbance as an indicator of the chemical composition and reactivity of dissolved organic carbon. Environ. Sci. Technol. **37**: 4702–4708. doi:10.1021/es030360x

Wilkinson, G. M., S. R. Carpenter, J. J. Cole, and M. L. Pace. 2014. Use of deep autochthonous resources by zooplankton: Results of a metalimnetic addition of ^{13}C to a small lake. Limnol. Oceanogr. **59**: 986–996. doi:10.4319/lo.2014.59.3.0986

Williamson, C. E., E. P. Overholt, R. M. Pilla, T. H. Leach, J. A. Brentrup, L. B. Knoll, E. M. Mette, and R. E. Moeller. 2015. Ecological consequences of long-term browning in lakes. Sci. Rep. **5**: 18666. doi:10.1038/srep18666

Wrona, F. J., and others. 2016. Transitions in Arctic ecosystems: Ecological implications of a changing hydrological regime. J. Geophys. Res. Biogeosci. **121**: 650–674. doi:10.1002/2015JG003133

Xiao, Y.-H., T. Sara-Aho, H. Hartikainen, and A. V. Vähätalo. 2013. Contribution of ferric iron to light absorption by chromophoric dissolved organic matter. Limnol. Oceanogr. **58**: 653–662. doi:10.4319/lo.2013.58.2.0653